

Laser Photolysis of Hemochromes. Kinetics of Nitrogenous Bases Binding to Four-Coordinated and Five-Coordinated Iron(II) Tetraphenylporphine

Daniel Lavalette,* Catherine Tetreau, and Michel Momenteau

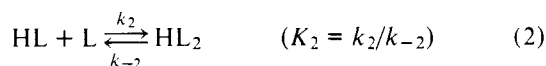
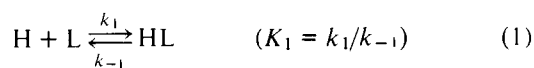
Contribution from Institut Curie, Section de Biologie, Fra No. 25 de l'Inserm, Centre Universitaire, Bâtiment 112, 91405 Orsay, France. Received January 29, 1979

Abstract: Six-coordinated complexes of iron(II) porphyrins with nitrogenous bases as axial ligands (hemochromes) can be photodissociated by a laser pulse. The photodissociation of hemochromes has been used in order to investigate the reactivity of a number of nitrogenous bases toward iron(II) tetraphenylporphyrin and two derived compounds in which one base (imidazole or pyridine) is covalently linked to the porphyrin macrocycle (chelated models). The recombination of photodissociated hemochromes exhibits a variety of kinetic patterns, which are attributed to the spontaneous dissociation of the unstable five-coordinated species formed upon photolysis. The rate constants for axial ligand binding and dissociation are found to decrease upon increasing the pK_a of the external ligand, in contrast to the opposite pK_a dependence of the equilibrium constants. Examination of the potential energy terms governing the reaction rates suggests that electrostatic repulsion between ligand and five-coordinated porphyrin dipole moments might account for the variation of the association rate constant.

Introduction

The ability of iron(II) porphyrins to form six-coordinated complexes with nitrogenous bases as ligands has long been recognized, and the chemical and physical properties of these complexes (hemochromes) have been investigated extensively.¹⁻⁹

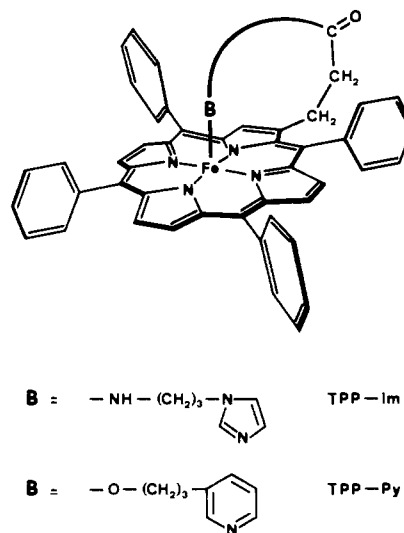
The binding of a nitrogenous base L to a four-coordinated iron(II) porphyrin H is thought to proceed in two steps (eq 1 and 2). With few exceptions,^{5,10} only the overall reaction is observed at equilibrium, and six-coordinated HL_2 (i.e., the hemochrome) is the dominant species in solution. This is taken as evidence that the equilibrium constant K_1 is much smaller than K_2 .^{2,3} One of the axial bases of hemochromes can be exchanged with carbon monoxide, and the kinetics of this replacement has been studied using rapid mixing¹¹⁻¹⁴ or flash photolysis techniques.¹⁵⁻¹⁹ However, the kinetic rate constants of hemochrome formation and dissociation as defined in eq 1 and 2 remained unknown.



In a preliminary report,²⁰ we have shown that hemochromes may be photodissociated by a laser pulse. Photodissociation produces five-coordinated HL as the primary species with a quantum yield lying in the range 10^{-1} to 10^{-2} and is followed by the fast recombination of one ligand molecule with a rate constant on the order of $10^8 \text{ M}^{-1} \text{ s}^{-1}$. Thus, photodissociation can be used as a trigger perturbation of the equilibria 1 and 2 in order to directly investigate the reactivity of the ligands.

In the present work, we have determined some of the four rate constants governing the complexation of a number of nitrogenous bases with iron(II) meso- $\alpha,\beta,\gamma,\delta$ -tetraphenylporphine ($\text{Fe}^{\text{II}}\text{TPP}$) and two derived compounds in which one base B (imidazole or pyridine) is covalently linked to the TPP macrocycle ($\text{Fe}^{\text{II}}\text{TPP-B}$).

These compounds are analogues in the TPP series of the chelated heme models introduced by Traylor and co-workers.²¹ In the following, it will be useful to distinguish external ligands (L), which are simply added to $\text{Fe}^{\text{II}}\text{TPP}$ in solution, and chelated ligands (-B), which are covalently attached to the porphyrin. The resulting hemochromes are represented by $(L)_2\text{Fe}^{\text{II}}\text{TPP}$ and $(L)\text{Fe}^{\text{II}}\text{TPP-B}$, respectively, in which (L) refers



to nitrogenous bases only. Complexes involving carbon monoxide and a chelated heme are denoted $(\text{CO})\text{Fe}^{\text{II}}\text{TPP-B}$.

Experimental Section

Products. Ferric complexes of TPP, TPP-Im, and TPP-Py were synthesized and purified according to published procedures.²²⁻²⁴

Imidazole (Im), 1-methylimidazole (1-MeIm), pyridine (Py), 4-cyanopyridine (4-CNPy), 4-acetylpyridine (4-AcPy), 4-methylpyridine (4-MePy), 4-dimethylaminopyridine (4-NMe₂Py) (all from Aldrich), and piperidine (Pip) (Fluka) were recrystallized or distilled just before use. 4-Chloropyridine (4-ClPy) was obtained from Cilab-Chemie as the hydrochloride. It was dissolved in aqueous sodium hydroxide, extracted with chloroform, dried over Na_2SO_4 , collected by evaporation of the solvent, and rapidly distilled under reduced pressure. During the distillation an important part of the compound polymerized, due to the formation of solid pyridinium derivatives.²⁵ Solutions of 4-ClPy in toluene were prepared immediately and stored at -40°C .

Argon and carbon monoxide were from "l'Air Liquide" ($\text{O}_2 < 5 \text{ ppm}$). The solubility of CO in toluene was taken as $7.3 \times 10^{-3} \text{ M}$ (25°C , 1 atm).²⁶

Preparation of Samples. The ferrous porphyrins were prepared in toluene solutions from ferric chloride complexes according to the method described elsewhere.^{3,27} The hemins ($5 \times 10^{-5} \text{ M}$) were reduced by aqueous sodium dithionite under an atmosphere of toluene-saturated argon (or carbon monoxide for the CO-exchange experiments). The optical cell ($5 \times 10 \text{ mm}$) was first flushed using the

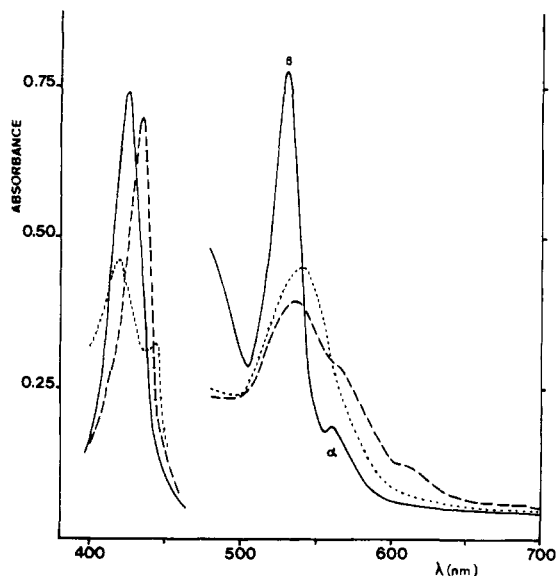


Figure 1. Absorption spectrum of four-coordinated $\text{Fe}^{\text{II}}\text{TPP}$ (---), five-coordinated $\text{Fe}^{\text{II}}\text{TPP-Py}$ (···), and hemochrome (Py) $\text{Fe}^{\text{II}}\text{TPP-Py}$ (—) in toluene. Concentration, 4×10^{-5} M; optical path, 10 mm in the visible and 1 mm in the Soret region.

desired gas. One-hundred microliters of a previously deaerated ligand solution was introduced by means of a syringe through a latex septum, and the required amount of reduced $\text{Fe}(\text{II})$ porphyrin solution was then transferred into the cuvette. All measurements were performed at constant temperature (25 °C). The ligand was always present in a large excess in order to warrant complete hemochrome formation and to satisfy pseudo-first-order kinetics.

Kinetic Measurements. Laser photolysis was performed using the second harmonic (530 nm) of a Q-switched neodymium laser (Quantel). The pulse had a width of 20 ns and its energy could be varied between 1 and 50 mJ. The monitoring light was provided by a xenon arc (Osram, 75 W) that was pulsed for 1 ms to about 200 times its nominal brightness, in order to achieve the high signal-to-noise ratio required for recording small absorbance changes in single shot experiments on a fast time scale (100 ns to 100 μs). Alternatively, the light of a continuously running quartz-iodine lamp (Osram, 100 W) could be directed toward the sample by means of a total reflection prism without disturbing the alignment. This arrangement allowed us to record slower transients, as in the CO-exchange experiments (from 100 μs up to several seconds). The collimated light beam crossed the sample at a right angle to the laser direction, and the emerging light entered a grating monochromator (Hilger and Watts, 600 grooves/mm). A 1P28 (RCA) photomultiplier operated with five dynodes only was used as detector and could deliver up to 3 mA in the pulsed-mode operation. The signal was displayed on a Tektronix 549 Storage oscilloscope. Absorbance changes were monitored at the wavelength of the hemochrome β band (527–535 nm) (Figure 1). Because of the strong absorbance in the Soret region and the high quantum yield of photolysis of $(\text{CO})\text{Fe}^{\text{II}}\text{TPP-B}$ complexes, the samples were protected by a cut-off filter (λ transmitted >450 nm).

Results

I. Chelated Models: $(\text{L})\text{Fe}^{\text{II}}\text{TPP-B}$. The results obtained with the chelated models will be presented first, as the chemically simpler $(\text{L})_2\text{Fe}^{\text{II}}\text{TPP}$ complexes exhibit a more complicated behavior. The stable five-coordinated $\text{Fe}^{\text{II}}\text{TPP-B}$ can react with a series of ligands and, since the chelated base B is either imidazole or pyridine, its influence on the reaction rates can be investigated.

a. Recombination Rates: k_2 . The primary species formed immediately after photolysis of $(\text{L})\text{Fe}^{\text{II}}\text{TPP-B}$ has been shown to be the five-coordinated $\text{Fe}^{\text{II}}\text{TPP-B}$ complex.²⁰ Since the ligand concentration, $[\text{L}]$, is always much greater than the total heme concentration, $[\text{H}_{\text{tot}}]$, all bimolecular reactions involving one external ligand follow pseudo-first-order kinetics. The time

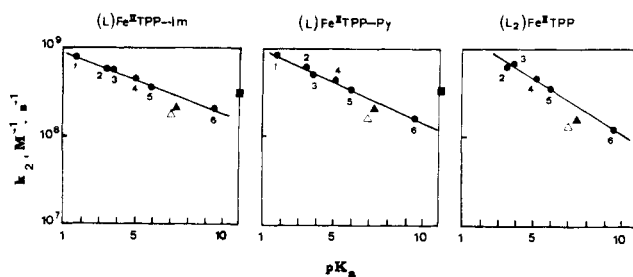


Figure 2. Rate constant k_2 for the recombination of the external ligand following photodissociation of $(\text{L})_2\text{Fe}^{\text{II}}\text{TPP}$ and $(\text{L})\text{Fe}^{\text{II}}\text{TPP-B}$ hemochromes as a function of ligand basicity. The ligands are: (●) 4-CNPY (1), 4-AcPy (2), 4-ClPy (3), Py (4), 4-MePy (5), and 4-NMe₂Py (6); (▲) Im; (▲) 1-Melm; (■) Pip; (□) $\text{Fe}^{\text{II}}\text{TPP-B}$, directly measured k_2 values; (○) $(\text{L})_2\text{Fe}^{\text{II}}\text{TPP}$, asymptotic value of " k_{on} " (see Figure 6).

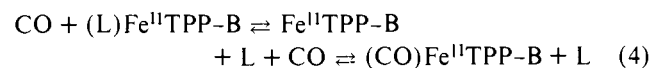
evolution of the absorbance change ΔA during the recombination is then given by:

$$\Delta A/\Delta A_0 = \exp(-k_2[\text{L}]t) = \exp(-t/\tau) \quad (3)$$

This relation was obeyed over the whole range of ligand concentrations²⁸ (5×10^{-4} to 5×10^{-2} M), allowing an accurate determination of k_2 for a number of bases. The results are summarized in Figure 2, in which $\ln k_2$ is plotted against the $\text{p}K_a$ value of the external base.

Within a series of chemically related bases (e.g., para-substituted pyridines), an excellent correlation of the reaction rate with the $\text{p}K_a$ is observed. Ligands with a different chemical structure do not fit the correlation so well.

b. Spontaneous Dissociation Rates: k_{-2} . The "off" rates k_{-2} were determined using $(\text{CO})\text{Fe}^{\text{II}}\text{TPP-B}$ complexes, which are stable even in the presence of a large excess of a free base L.²⁹ Carbon monoxide complexes were easily photodissociated, and the direct recombination of CO was found to take place with rate constants $k_{\text{CO}} = 4.5 \times 10^6 \text{ M}^{-1} \text{ s}^{-1}$ for $\text{Fe}^{\text{II}}\text{TPP-Im}$ and $k_{\text{CO}} = 6.6 \times 10^6 \text{ M}^{-1} \text{ s}^{-1}$ for $\text{Fe}^{\text{II}}\text{TPP-Py}$. Since the rate constant k_2 is much larger for the nitrogenous bases, the conditions can be adjusted such that L recombine first with the five-coordinated $\text{Fe}^{\text{II}}\text{TPP-B}$, giving rise to the transient formation of hemochrome and initiating the exchange reaction:



The rate of exchange, θ , is given by Gibson's equation:³⁰

$$\theta = ((1 + k_2[\text{L}])/k_{\text{CO}}[\text{CO}])/k_{-2} \quad (5)$$

In terms of the exponential time constants τ_{L} and τ_{CO} for the reaction of the ligand and of carbon monoxide (see eq 3), the parentheses may be rewritten as $(1 + \tau_{\text{CO}}/\tau_{\text{L}})$. The direct measurement of θ and τ_{L} using a single sample is shown in Figure 3.

The results are given in Figure 4. The intrinsic stability, as characterized by k_{-2} , increases with the ligand $\text{p}K_a$ and is about three times more sensitive to $\text{p}K_a$ changes than k_2 . Piperidine, 4-CNPY, and 4-AcPy deviate significantly from the correlation.

c. Equilibrium Constants: K_2 . The equilibrium constants for the fixation of the second (external) base ($K_2 = k_2/k_{-2}$) were calculated from the above results and are plotted as a function of $\text{p}K_a$ in Figure 5. Of course, K_2 values reproduce the deviations already found either for k_2 or k_{-2} . In particular, the affinity of 4-CNPY and 4-AcPy appears to be too high, that of piperidine too low.

II. Symmetrical Hemochromes: $(\text{L})_2\text{Fe}^{\text{II}}\text{TPP}$. The recombination rate constant after photolysis of $(\text{L})_2\text{Fe}^{\text{II}}\text{TPP}$ hemochromes was found in most cases to be a function of the base

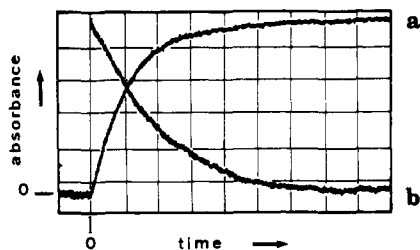


Figure 3. Photolysis of $(\text{CO})\text{Fe}^{\text{II}}\text{TPP-Py}$ ($5 \times 10^{-5} \text{ M}$) in the presence of free 4-CNPy (10^{-3} M) ($[\text{CO}] = 7.3 \times 10^{-3} \text{ M}$), monitored at the absorption maximum of $(4\text{-CNPy})\text{Fe}^{\text{II}}\text{TPP-Py}$ (532 nm). (Trace a) Transient formation of $(4\text{-CNPy})\text{Fe}^{\text{II}}\text{TPP-Py}$ hemochrome, 1 μs /division. Since $(\text{CO})\text{Fe}^{\text{II}}\text{TPP-Py}$ and its initial photolysis product $\text{Fe}^{\text{II}}\text{TPP-Py}$ are practically isosbestic at this wavelength, the absorbance change $\Delta A = 0$ at $t = 0$ and then increases, due to the fast build-up of a hemochromic population. (Trace b) Exchange of the hemochromic external ligand (4-CNPy) with CO. 1 ms/division. The hemochrome $(4\text{-CNPy})\text{Fe}^{\text{II}}\text{TPP-Py}$ is not stable in the presence of a high concentration of carbon monoxide. A slow exchange takes place, restoring the initial $(\text{CO})\text{Fe}^{\text{II}}\text{TPP-Py}$. Absorbance scale, 0.01/division.

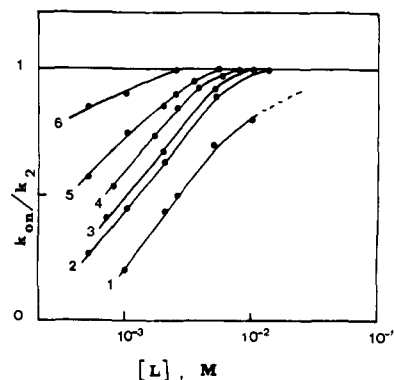


Figure 6. Recombination of the second external base of photodissociated $(\text{L})_2\text{Fe}^{\text{II}}\text{TPP}$ hemochromes: relative value of the apparent recombination rate constant (k_{on}) as a function of ligand concentration. The numbers refer to the ligands as defined in Figure 2.

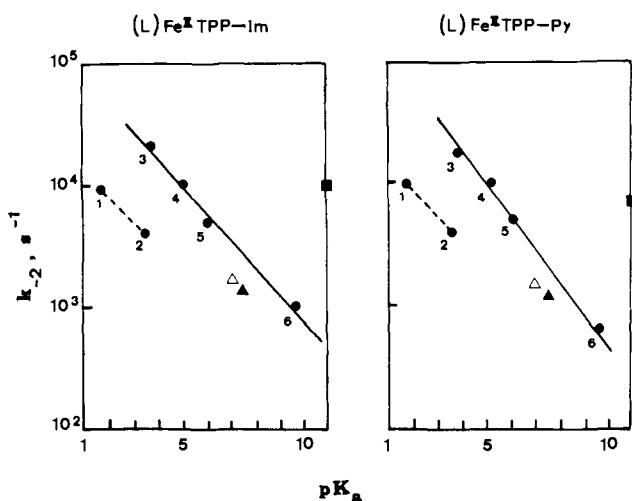


Figure 4. Rate constant k_{-2} for the spontaneous dissociation of the external ligand in $(\text{L})\text{Fe}^{\text{II}}\text{TPP-B}$ hemochromes as a function of ligand basicity, determined from exchange experiments with carbon monoxide. The ligands are as in Figure 2.

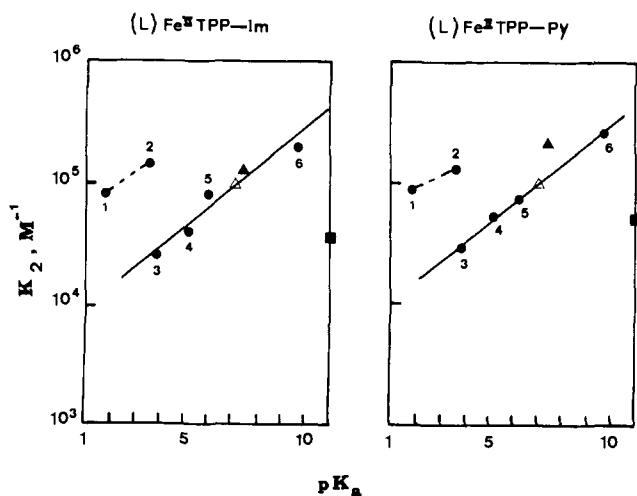


Figure 5. Calculated equilibrium constant ($K_2 = k_2/k_{-2}$) for the binding of the external ligand of $(\text{L})\text{Fe}^{\text{II}}\text{TPP-B}$ hemochromes as a function of ligand basicity. The ligands are as in Figure 2.

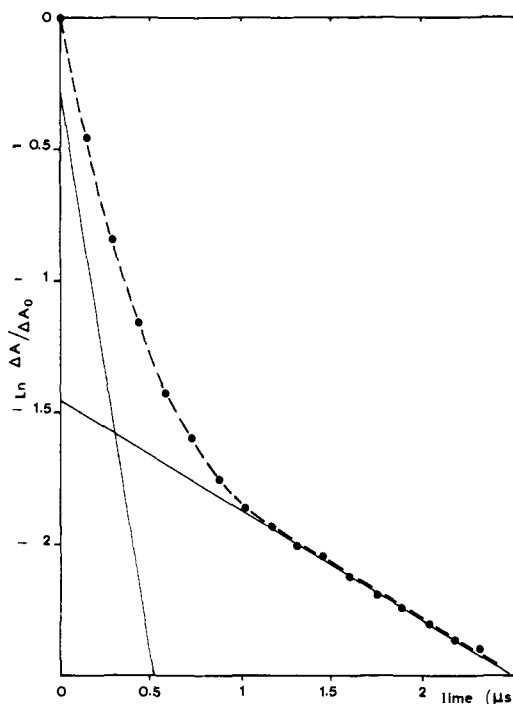


Figure 7. Logarithmic plot of the relative absorbance change $\Delta A/\Delta A_0$, following photodissociation of $(\text{pip})_2\text{Fe}^{\text{II}}\text{TPP}$. The dashed line is drawn through the experimental points. This nonexponential decay was resolved into two exponentials (full lines) using nonlinear regression analysis.

concentration $[\text{L}]$. In order to avoid confusion, we shall call " k_{on} " this apparent, concentration-dependent rate constant. Three different situations were observed, depending on the nature of the external ligands.

a. Imidazole and 1-MeIm. k_{on} remained constant over the whole range of ligand concentration ($5 \times 10^{-4} \text{ M} < [\text{L}] < 2 \times 10^{-2} \text{ M}$).

b. Pyridine and Para-Substituted Derivatives. k_{on} was found to increase with $[\text{L}]$ up to a constant value at high concentration (Figure 6). However, semilog plots of the absorbance changes did not exhibit any significant deviation from a single exponential.

c. Piperidine. The recombination kinetics of piperidine hemochromes was distinctly biphasic (Figure 7).

The fact that such deviations did not occur with the chelated models suggested that the stability of the five-coordinated species formed upon photolysis was probably involved. It is well

known that five-coordinated Fe(II) porphyrins are not stable in solution;³ photogenerated HL must therefore disappear, either by reaction with one ligand molecule to restore the hemochrome, or by spontaneous dissociation to give a bare heme.¹⁷ Three species must therefore be considered in order to account for the reassociation kinetics.

From eq 1 and 2 we have:

$$\frac{d[H]}{dt} = -k_1[L][H] + k_{-1}[HL] \quad (6)$$

$$\frac{d[HL]}{dt} = k_1[L][H] - (k_{-1} + k_2[L])[HL] + k_{-2}[HL_2] \quad (7)$$

$$\frac{d[HL_2]}{dt} = k_2[L][HL] - k_{-2}[HL_2] \quad (8)$$

This system can be solved using the pseudo-first-order approximation $[L] > [H]_{\text{tot}}$ and neglecting the terms involving k_{-2} in view of the stability of hemochromes in solution. The recombination of hemochromes is now found to be generally biphasic:

$$\frac{[HL_2]_t - [HL_2]_e}{[HL_2]_0 - [HL_2]_e} = C^+ \exp(r^+t) + C^- \exp(r^-t) \quad (9)$$

where the subscripts denote the equilibrium and the initial ($t = 0$) concentrations, respectively,³¹ and where r^+ and r^- are a slow and a fast rate given by:

$$r^\pm = \frac{1}{2} \left\{ -[(k_1 + k_2)[L] + k_{-1}] \pm [(k_1 + k_2)[L] + k_{-1}]^2 - 4k_1k_2[L]^2 \right\}^{1/2} \quad (10)$$

In order to simplify the discussion, it is useful to introduce the dimensionless parameters:

$$x = K_1[L] \quad (11)$$

$$\alpha = k_1/k_2 \quad (12)$$

Equation 10 then transforms into:

$$r^\pm = \frac{k_2[L]}{2} \left\{ -(\alpha + 1 + \alpha/x) \pm [(\alpha + 1 + \alpha/x)^2 - 4\alpha]^{1/2} \right\} \quad (13)$$

The weight factors C^+ and C^- of the slow and fast rates are given by the relations:

$$C^+ + C^- = 1 \quad (14)$$

and

$$C^+/C^- = -(r^-/r^+) \left((r^+ + k_1[L]) / (r^- + k_1[L]) \right) \quad (15)$$

Figure 8 presents a graphical discussion of the various kinetics that can be expected as a function of ligand concentration and strength. At high ligand concentration, the observed rate will always become identical with k_2 . This corresponds to the asymptotic value of k_{on} in Figure 6. Two limiting cases are of interest: $-\alpha > 1$, the fast rate has a small weight (in practice, only the slow rate can be observed and should decrease at low ligand concentration (Figure 8a)); $-\alpha < 1$, a dual exponential can eventually be observed, since the rates are significantly different, but both components appear with large contributions (Figure 8c).

The significance of a recombination rate faster than $k_2[L]$ is best understood by considering the total rate of disappearance of HL, which, at $t = 0$, is equal to: $k_2[L] + k_{-1}$ (see eq 7). A fraction $k_2[L]/(k_2[L] + k_{-1})$ will re-form hemochrome by direct association, and the remaining fraction $k_{-1}/(k_2[L] + k_{-1})$ will dissociate to give a bare heme. Thus, the fast rate

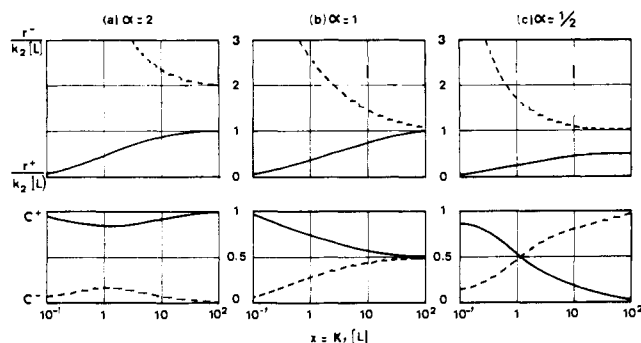


Figure 8. Graphical discussion of the solutions of eq 6 to 8 governing the recombination kinetics of $(L)_2\text{Fe}^{\text{II}}\text{TPP}$ hemochromes. (Top) Relative values of the slow (—) and fast rate (---) as a function of the dimensionless parameter $x = K_1[L]$. (Bottom) Weight factors C^+ and C^- associated with the slow (r^+) and fast rate (r^-), respectively. The graphs were established according to eq 13 and 15 for three values of the parameter $\alpha = k_1/k_2$. The critical dependence of C^+ and C^- on α determines the different kinetics discussed in the text.

corresponds to those hemochromes that recombine during the shortened lifetime of HL. The slow rate involves the successive addition of two ligands to the free heme and must be therefore slower than $k_2[L]$.

Though introducing some complexity, the dissociation of the five-coordinated intermediate HL permits us to analyze the experimental results:

1. 1-MeIm Is a Strong Ligand. $K_1 = 6 \times 10^4 \text{ M}^{-1}$.²⁴ In the concentration range $5 \times 10^{-4} \text{ M} < [L] < 2 \times 10^{-2} \text{ M}$, one has $30 < x < 600$ and only a single exponential with a rate constant equal to k_2 can be observed for any value of α (Figure 8).

2. Pyridine and Derivatives. A value of $K_1 = 1.5 \times 10^3 \text{ M}^{-1}$ has been reported for $(\text{Py})_2\text{Fe}^{\text{II}}\text{TPP}$ in benzene.³ Therefore, $0.5 < x < 10$. Since only single exponentials were observed in the recombination experiments, one should have $\alpha > 1$ (Figure 8). Attempts to fit the curves of Figure 6 to the value of the slow rate given by eq 13 using nonlinear regression analysis were not satisfactory. It was found that k_{on} reached its asymptotic value at concentrations lower than expected. This failure can be understood if $k_1 \sim k_2$ in the pyridine series. As shown in Figure 8b, the values of the slow and fast rate, as well as their weight factors, diverge only slowly over a wide range of x . Their superposition is likely to simulate an average exponential recombination with a rate constant practically equal to the asymptotic k_2 . The concentration dependence of k_{on} is therefore distorted, preventing a safe quantitative analysis. However, the results of Figure 6 show that the first equilibrium constant K_1 must decrease in this series in the order: 4-NMe₂Py > 4-MePy > Py > 4-ClPy > 4-AcPy > 4-CNPpy, i.e., in the order of decreasing $\text{p}K_a$ as found previously for K_2 . For all para-substituted pyridines, the asymptotic k_{on} was found to be equal within about 20% to the value of k_2 obtained with the chelated models.³²

3. Piperidine. The biexponential recombination of $(\text{pip})_2\text{Fe}^{\text{II}}\text{TPP}$ (Figure 7) was easily resolved by nonlinear regression analysis into: $r^+ = -4.16 \times 10^5 \text{ s}^{-1}$ ($C^+ = 0.24$) and $r^- = -4.27 \times 10^6 \text{ s}^{-1}$ ($C^- = 0.76$) for $[\text{pip}] = 10^{-2} \text{ M}$. From eq 15, we estimated $k_1 = 5.3 \times 10^7 \text{ M}^{-1} \text{ s}^{-1}$. The constants k_2 and k_{-1} (Table I) were obtained using the additional relations:

$$r^+r^- = k_1k_2[L]^2 \quad (16)$$

and

$$|r^+| + |r^-| = (k_1 + k_2)[L] + k_{-1} \quad (17)$$

The calculated value of k_2 is in agreement with that measured using the chelated $(\text{pip})\text{Fe}^{\text{II}}\text{TPP-Py}$ (Table I).

Thus, for all the investigated ligands, k_2 was found to be

Table I. Rate and Equilibrium Constants of Hemochromes for Three Representative Ligands, Determined Using Fe^{II}TPP or Chelated Fe^{II}TPP-Im and Fe^{II}TPP-Py

	l-methylimidazole		pyridine		piperidine	
	Fe ^{II} TPP	Fe ^{II} TPP-Im	Fe ^{II} TPP	Fe ^{II} TPP-Py	Fe ^{II} TPP	Fe ^{II} TPP-Py
k_1 (M ⁻¹ s ⁻¹)					5.3×10^7	
k_{-1} (s ⁻¹)					8×10^5	
k_2 (M ⁻¹ s ⁻¹)	1.6×10^8	1.8×10^8	4.5×10^8	4.7×10^8	3.4×10^8	3.7×10^8
k_{-2} (s ⁻¹)		1.5×10^3		1.2×10^4		7.5×10^3
K_1 (M ⁻¹)	(6×10^4)		(1.5×10^3)		66	
K_2 (M ⁻¹)	(1.4×10^5)	1.2×10^5	(2.4×10^4)	3.7×10^4		4.9×10^4

^a The equilibrium constants in parentheses are from ref 3 and 24. Solvent, toluene; temperature, 25 °C.

almost the same for (L)₂Fe^{II}TPP and (L)Fe^{II}TPP-B complexes (Table I). In view of the complications introduced by the dissociation of HL in the presence of competing ligands, a direct determination of k_{-2} using the CO exchange technique was not attempted with (L)₂Fe^{II}TPP hemochromes.

Discussion

The spontaneous dissociation of photogenerated five-coordinated (L)Fe^{II}TPP is responsible for the complexity of the reassociation kinetics of the external ligand to restore (L)₂-Fe^{II}TPP hemochromes. This mechanism, which may be quite general for metalloporphyrins with $K_1 < K_2$, is the same as that found by Cannon et al.¹⁷ in a study of the reaction of hemo-protein models with carbon monoxide, and called by them "the base elimination pathway". The present treatment shows that the reassociation kinetics is governed by K_1 and k_1 , two constants which are generally not known. Although their estimation was possible only in the case of the biexponential kinetics of (pip)₂Fe^{II}TPP, some semiquantitative statements may be made for the pyridine series. Thus, K_1 increases regularly with the base pK_a and $k_1 \approx k_2 \approx 5 \times 10^8$ M⁻¹ s⁻¹.

The systematic study of the rate constants k_2 and k_{-2} using chelated (L)Fe^{II}TPP-Py and (L)Fe^{II}TPP-Im has shown that the relation between rate (and equilibrium) constants and the pK_a of the external base takes the form of Hammett's rules: $\ln k_i = \rho_i(pK_a) + \text{constant}$. The slopes are quite similar for Fe^{II}TPP-Im and Fe^{II}TPP-Py complexes: $\rho_2 = -0.18$ and -0.22 , $\rho_{-2} = -0.54$ and -0.62 , respectively. Thus, the "trans effect" exerted by the chelated base upon the fixation of the sixth external ligand is rather small, in comparison with the variations of the rate constant due to the intrinsic properties of the external base. That the reaction rates are primarily governed by the external base is further shown by the comparison of nonsymmetrical hemochromes in which the role of the chelated and external base is interchanged (Table II).

The reactivity of CO and O₂ with iron(II) porphyrins is still being investigated in great detail because of its obvious interest for understanding the properties of oxygen carrier hemoproteins. In contrast, investigations concerning the reactivity of the nitrogenous bases are very scarce. The fast reaction rates (10^8 to 10^9 M⁻¹ s⁻¹) as compared to carbon monoxide (10^6 to 10^7 M⁻¹ s⁻¹) and the lower quantum yield (0.1 to 0.01) probably explain why the photodissociation of hemochromes has remained unobserved up to now.^{33,34} Laser photolysis of heme (CO)(Im) complexes was carried out recently by White et al.,¹⁹ who indirectly estimated $k_2 \approx 10^8$ M⁻¹ s⁻¹ and $k_{-2} \approx 1500$ s⁻¹ for imidazole and deuteroporphyrin dimethyl ester in benzene, in good agreement with the present results. On the other hand, rapid mixing techniques have been used previously for obtaining k_{-2} from CO-external base exchange rates. A value of $k_{-2} = 11$ s⁻¹ reported for (pip)₂Fe^{II}TPP^{11,12} is almost three orders of magnitude slower than that measured by us. As pointed out by White et al.,¹⁹ these experiments ignored the spontaneous dissociation of the five-coordinated species. Our k_2 and k_{-2} values lead to equilibrium constants K_2 that are in

Table II. Effect of Interchange of Chelated and External Bases on the Kinetic Rate Constants of Fe^{II}TPP Hemochromes in Toluene (25 °C)

	(Im)Fe ^{II} - TPP-Im	(Im)Fe ^{II} - TPP-Py	(Py)Fe ^{II} - TPP-Im	(Py)Fe ^{II} - TPP-Py
k_2 (M ⁻¹ s ⁻¹)	1.9×10^8	1.6×10^8	4.5×10^8	4.7×10^8
k_{-2} (s ⁻¹)	1.7×10^3	1.5×10^3	1.2×10^4	1.2×10^4

good agreement with those obtained independently by a direct titration in the few cases where K_1 and K_2 could be measured separately^{3,24} (see Table I).

It may be questioned whether the presence of about 3×10^{-2} M of H₂O in wet toluene might have vitiated the rate constant measurements, since water has a small but noticeable affinity for five-coordinated species ($K_{H_2O}^{CO} \approx 10$ M⁻¹).²⁹ At the high ligand concentration used, hemochrome reassociation was completed within about 500 ns to 1 μs. Thus, a rate constant $k_{H_2O} \gg 3 \times 10^9$ M⁻¹ s⁻¹ should be required in order for water to interfere with ligand recombination. After we bubbled dry CO for 20 min through (CO)Fe^{II}TPP-B + L mixtures, the rate constant k_2 remained unchanged within experimental error. Since this procedure is known to reduce the water concentration by a factor of ten,²⁹ we may conclude that H₂O does not compete with ligand fixation in our experiments. The good agreement between the equilibrium constants K_2 derived from the kinetic measurements and those measured directly and found in the literature further supports the above conclusion, since the role of water in hemochrome equilibria has been shown to be negligible.⁹

The variations of k_2 , k_{-2} , and K_2 upon changing the external base depend on several factors, which can be discussed in light of the theory of absolute reaction rates. For a series of similar reactions such as those considered here, it is usually assumed that ratios of partition functions remain constant and that the relative values of the rate constants are mainly governed by energy terms.

Equilibrium and Dissociation Constants: K_2 and k_{-2} . Both constants depend on the ground-state energy of the final complex. Nitrogenous bases are generally considered to add by σ bonding to the metal in d⁶ low-spin systems; there seems to be no general agreement concerning a π back-bonding contribution from the d_π iron orbitals to an antibonding π^* ligand orbital. To the extent that pK_a may reflect the availability of the nitrogen lone-pair electrons for σ bonding, an increase of $\ln K_2$ with pK_a is not surprising. Both equilibrium constants K_1 and K_2 for the binding of pyridines to ferrous phthalocyanine in dimethyl sulfoxide⁶ as well as the enthalpy for the binding of two ligands to various Fe(II) porphyrins,⁷ have been reported to follow similar correlations. However, 4-CNPy, 4-AcPy, and 4-carboxybutylpyridine were found to be systematically more stable than their σ donor capacity would indicate. Thus, Cole et al.⁷ suggest that σ bonding predominates at the high end of the pK_a scale, but that a π -bonding contribution tends to strengthen the bond as pK_a de-

creases. The same exceptions to the linear relationship between $\ln K_2$ and pK_a have been observed in this work, but their origin is found in the low dissociation rate constant k_{-2} , while k_2 remains unaffected (Figures 2 and 4). The increased stability of 4-CNPy and 4-AcPy does not apparently result from their low pK_a only, since 4-ClPy follows the correlation, in spite of having a pK_a almost equal to that of 4-AcPy. Indications about the nature of the additional stabilization energy in these complexes are given by their adsorption spectrum. (4-CNPy)Fe^{II}TPP-B and (4-AcPy)Fe^{II}TPP-B hemochromes present a new absorption band around 700 nm, which resembles a charge-transfer transition, although its exact nature has not yet been established.²⁴ Hence, it is tempting to speculate that a small amount of charge transfer might be responsible for the increased stability of these hemochromes.

On the contrary, piperidine complexes are less stable than one would expect in view of the donor power of the base (Figure 5). The reasons may be the inability of piperidine to accept π electrons, in addition to the steric repulsion that increases the Fe-N bond length by 0.15 Å, as compared to the imidazole ligand.³⁵

The contribution of π bonding in the pyridine series is perhaps related to the yield of photodissociation. In their study on the photosensitivity of liganded hemes, Hoffman and Gibson,³³ referring to previous work,³⁴ consider low-spin six-coordinated ferroporphyrin complexes as photostable. They further suggest that, if π bonding does not contribute to the Fe-L bond strength, photoexcitation of an antibonding $\pi-\pi^*$ state of the porphyrin should not cause the photodissociation of L. Our own quantum yield measurements on a few TPP hemochromes gave $\phi = 0.03, 0.05,$ and 0.06 for piperidine, imidazole, and pyridine, respectively.²⁰ In the hypothesis of Hoffman and Gibson, the higher yield of pyridine could reflect a small contribution of π bonding at the lower pK_a . The same effect could explain the photostability of the five-coordinated (L)Fe^{II}TPP species.²⁰ If iron(II) is a poorer d_π donor in its high-spin state than in its low-spin state,³⁶ the amount of π bonding, and hence the photolability, should be lower in the five-coordinated complex.³⁷

Association Rate Constant: k_2 . The decrease of the association rate constant k_2 at higher pK_a (Figure 2) suggests that some pK_a -dependent part of the energy barrier limits the reaction rate. The use of pK_a as a guide for classifying the ligands with respect to their affinity may, however, become ambiguous for estimating the energy of the activated complex. Electrostatic, dispersion, and solvation terms are supposed to contribute to various extents to the energy barrier. Indeed, all the ligands we have investigated are strong dipoles (negative nitrogen), and the displacement of the iron atom about 0.5 Å away from the porphyrin plane in high-spin five-coordinated complexes³⁸ is likely to induce a dipole component along the fourfold (Z) symmetry axis (negative porphyrin nitrogens). Therefore, the approach of the external ligand to form the activated complex requires that enough kinetic energy must be supplied in order to overcome the electrostatic repulsion between the base dipole and the porphyrin charge distribution. We have noticed that the dipole moments μ of the bases are strongly correlated with their pK_a , increasing by about 0.4 D/ pK_a unit from $\mu = 1.6$ D (4-CNPy) to $\mu = 4.3$ D (4-NMe₂Py).³⁹ The only exception is piperidine, which has the highest pK_a and the smallest dipole moment (1.2 D), because of the absence of charge delocalization. Comparing piperidine and 4-NMe₂Py, its nearest neighbor in the pK_a scale, it is found that the former has the smallest equilibrium constant K_2 , but that its reaction rates k_2 and k_{-2} are faster than for 4-NMe₂Py, in spite of unfavorable steric constraints. This may be understood if electrostatic repulsion were contributing significantly to the energy barrier, which would then be lower for the smaller dipole, other things being equal.

The order of magnitude of the repulsion energy can be estimated by assuming that the charge distribution of the five-coordinated porphyrin can be approximated by a dipole moment component p along the Z axis. The repulsive interaction energy with the ligand dipole μ at a distance r is given by:⁴⁰

$$U = 2 \frac{\mu p}{r^3} \quad (18)$$

The variation of the rate constant due to the contribution of this energy term is:⁴¹ $\Delta \ln k_2 = -2p\Delta/kTr^3$, in which k is Boltzmann's constant and T is the absolute temperature. Using appropriate units and inserting the experimental values for $\Delta \ln k_2$, one obtains: $p/r^3 = 10^{-2}$, leading to an interaction energy $U = 0.3$ kcal mol⁻¹ per D of ligand dipole. The Arrhenius activation energy, $E_a = U + RT$,⁴¹ is then about 1.1 kcal mol⁻¹ for pyridine ($\mu = 2.2$ D). In this work, systematic measurements of the activation energy were not made, but preliminary results obtained with (Py)Fe^{II}TPP-Py over a limited temperature range (10 to 30 °C) gave $E_a \approx 2.9$ kcal mol⁻¹. Thus, the dipole-dipole energy term would contribute to roughly one-third of the total energy barrier. Measurements of the dipole moment of five-coordinated Fe^{II}TPP-Py and Fe^{II}TPP-Im are required in order to test further this hypothesis. Using the extended Hückel method, Zerner et al.⁴² have calculated the charge distribution in a five-coordinated ferrous porphyrin with a water molecule at the fifth coordination position of the iron. From their results, a value of 3 to 4 D for the dipole moment component along the Z axis seems acceptable. If this were the case for our Fe^{II}TPP-B complexes, and using $p/r^3 = 10^{-2}$, the average center to center distance of the dipoles at the peak of the barrier would be about 7 Å. The above estimations are not meant to imply that electrostatic repulsion is the only energy term to be considered for evaluating the energy barrier, but that this term is of the correct order of magnitude to account for the variations of k_2 with the pK_a of the external base.

Acknowledgment. The authors thank Dr. Mispelter for kindly performing the nonlinear least-squares analysis.

References and Notes

- J. E. Falk, "Porphyrins and Metalloporphyrins", Elsevier, Amsterdam, 1964.
- D. Brault and M. Rougee, *Biochem. Biophys. Res. Commun.*, **57**, 654-659 (1974).
- D. Brault and M. Rougee, *Biochemistry*, **13**, 4591-4597 (1974).
- J. P. Collman, J. L. Hoard, N. Kim, G. Lang, and C. A. Reed, *J. Am. Chem. Soc.*, **97**, 2676-2681 (1975).
- G. C. Wagner and R. J. Kassner, *Biochim. Biophys. Acta*, **392**, 319-327 (1975).
- J. G. Jones and M. W. Twigg, *Inorg. Chim. Acta*, **10**, 103-108 (1974).
- S. J. Cole, G. C. Curthoys, and E. A. Magnusson, *J. Am. Chem. Soc.*, **92**, 2991-2996 (1970).
- S. J. Cole, G. C. Curthoys, and E. A. Magnusson, *J. Am. Chem. Soc.*, **93**, 2153-2158 (1971).
- M. Momenteau, M. Rougee, and B. Loock, *Eur. J. Biochem.*, **71**, 63-76 (1976).
- J. P. Collman and C. A. Reed, *J. Am. Chem. Soc.*, **95**, 2048-2049 (1973).
- D. V. Stynes and B. R. James, *J. Chem. Soc., Chem. Commun.*, 325-326 (1973).
- D. V. Stynes and B. R. James, *J. Am. Chem. Soc.*, **96**, 2733-2738 (1974).
- C. J. Weschler, D. L. Anderson, and F. Basolo, *J. Chem. Soc., Chem. Commun.*, 757-758 (1974).
- C. J. Weschler, D. L. Anderson, and F. Basolo, *J. Am. Chem. Soc.*, **97**, 6707-6713 (1975).
- C. K. Chang and T. G. Traylor, *Proc. Natl. Acad. Sci. U.S.A.*, **72**, 1166-1170 (1975).
- J. Geibel, C. K. Chang, and T. G. Traylor, *J. Am. Chem. Soc.*, **97**, 5924-5926 (1975).
- J. Cannon, J. Geibel, M. Whipple, and T. G. Traylor, *J. Am. Chem. Soc.*, **98**, 3395-3396 (1976).
- J. Geibel, J. Cannon, D. Campbell, and T. G. Traylor, *J. Am. Chem. Soc.*, **100**, 3575-3585 (1978).
- D. K. White, D. H. Campbell, and T. G. Traylor, *J. Am. Chem. Soc.*, **101**, 2443-2454 (1979).
- M. Momenteau and D. Lavalette, *J. Am. Chem. Soc.*, **100**, 4322-4324

- (1978).
- (21) C. K. Chang and T. G. Traylor, *Proc. Natl. Acad. Sci. U.S.A.*, **70**, 2647–2650 (1973).
- (22) A. D. Adler, F. R. Longo, J. D. Finarelli, J. Assour, and L. Korsakoff, *J. Org. Chem.*, **32**, 476–481 (1967).
- (23) P. Rothermund and A. R. Menotti, *J. Am. Chem. Soc.*, **70**, 1808–1812 (1948).
- (24) M. Momenteau, B. Loock, E. Bisagni, and M. Rougee, *Can. J. Chem.*, in press.
- (25) H. S. Mosher, in "Heterocyclic Compounds", Vol. 1, R. C. Elderfield, Ed., Wiley, New York, 1950, p 516.
- (26) W. Linke and A. Seidell, "Solubilities of Inorganic and Metal-Organic Compounds", Van Nostrand, Princeton, N.J., 1958.
- (27) M. Momenteau, *Biochim. Biophys. Acta*, **304**, 814–827 (1973).
- (28) Photolysis of (1-Melm)Fe^{III}TPP-Im gave an initial, concentration-independent, short-lived decay (250 ns). It is believed that 1-Melm might have, in part, replaced Im at the fifth coordination position, due to its high K_1 value.²⁴ The short-lived decay would then correspond to the fast return of the chelated base Im.
- (29) M. Rougee and D. Brault, *Biochemistry*, **14**, 4100–4106 (1975).
- (30) R. W. Noble, Q. Gibson, M. Brunori, E. Antonini, and J. W. Wyman, *J. Biol. Chem.*, **244**, 3905–3908 (1969).
- (31) The left side of eq 9 can be identified with the absorbance changes measured at the hemochrome peak, although three species (HL₂, HL, and H) will be generally present during the recombination reaction. This approximation is justified in the present case since HL and H have almost identical absorbances at this wavelength (see Figure 1), thus reducing the number of kinetically distinct species.
- (32) The high k_2 of 4-CNPY prevented us from measuring the recombination rate at a very high concentration. In Figure 6 we have assumed that the asymptote was equal to the rate constant determined with (4-CNPY)-Fe^{III}TPP-Py.
- (33) B. M. Hoffman and Q. Gibson, *Proc. Natl. Acad. Sci. U.S.A.*, **75**, 21–25 (1978).
- (34) M. H. Smith, *Biochem. J.*, **73**, 90–101 (1959).
- (35) L. J. Radonovich, A. Bloom, and J. M. Hoard, *J. Am. Chem. Soc.*, **94**, 2073–2078 (1972).
- (36) B. B. Wayland, L. F. Mehne, and J. Swartz, *J. Am. Chem. Soc.*, **100**, 2379–2383 (1978).
- (37) We agree with a remark of one referee that because the Hoffman–Gibson hypothesis is of purely electronic character it does not take into account the possible contribution of dynamic factors such as energy relaxation and cage effects, which could also lead to a variation in the observed quantum yields. More extended data would be required, in order to clarify the question.
- (38) J. P. Collman, *Acc. Chem. Res.*, **10**, 265–272 (1977).
- (39) A. L. McClellan, "Tables of Experimental Dipole Moments", W. H. Freeman, San Francisco, 1963.
- (40) H. Eyring, J. Walter, and G. E. Kimball, "Quantum Chemistry", Wiley, New York, 1963, p 352.
- (41) R. Daudel, R. Lefebvre, and C. Moser, "Quantum Chemistry", Interscience, New York, 1959, pp 223–285.
- (42) M. Zerner, M. Gouterman, and H. Kobayashi, *Theor. Chim. Acta*, **6**, 363–400 (1966).

Ferric Ion Sequestering Agents. 2. Kinetics and Mechanism of Iron Removal from Transferrin by Enterobactin and Synthetic Triccatechols¹

Carl J. Carrano and Kenneth N. Raymond*

Contribution from the Department of Chemistry, University of California, Berkeley, California 94720. Received January 22, 1979

Abstract: The apparent first-order rate constants for iron removal from transferrin by the synthetic sequestering agents 1,5,10-*N,N',N''*-tris(5-sulfo-2,3-dihydroxybenzoyl)triazadecane (3,4-LICAMS), 1,3,5-*N,N',N''*-tris(2,3-dihydroxybenzoyl)aminomethylbenzene (MECAM), and the natural siderophore enterobactin (ent) have been determined at 25 °C. One of these compounds, 3,4-LICAMS, was examined in detail, and the mechanism of its removal of iron from transferrin elucidated. The 3,4-LICAMS ligand is observed to form a complex with transferrin prior to iron removal. The stability constant of this complex and the first-order rate constant for its dissociation to ferric LICAMS and apotransferrin are $K_{eq} = 4.1 (6) \times 10^2 \text{ M}^{-1}$ and $k_2 = 0.066 (4) \text{ min}^{-1}$, respectively. These results indicate that these catecholate ligands are both kinetically and thermodynamically capable of iron removal from transferrin at physiologically accessible concentrations. In contrast, the hydroxamate-based sequestering agents are kinetically hindered in this reaction. The implications of these results with respect to the possible use of these compounds as drugs in the treatment of iron overload syndromes are discussed.

Introduction

The treatment of certain blood disorders such as sickle cell anemia and β -thalassemia major requires chronic transfusion therapy. This regimen leads to an induced secondary hemochromatosis (buildup of iron in the tissues, particularly the heart, pancreas, and liver) causing fibrotic changes, and eventually failure of vital organs resulting in death.² This toxic buildup of iron results from the lack of a physiological mechanism in man for the excretion of this element. Attempts to remove excess iron from the body have led to a search for effective ferric ion chelating agents.³ The search originally centered on desferrioxamine B (Desferal), a hydroxamate siderophore produced by *Streptomyces pilosus*.^{4–6} Although Desferal is thermodynamically capable of removing iron from transferrin (the mammalian iron transport protein), its use in iron overload therapy has been only marginally successful. Desferal suffers from a series of drawbacks, among which are a lack of oral effectiveness, moderate toxicity, and, most important, the fact that it has not generally been possible to maintain patients in negative iron balance using this approach

without the need for long-term subcutaneous infusion therapy.^{7,8} Part of the ineffectiveness of Desferal stems from the fact that despite its high affinity for ferric ion, it is kinetically incapable, both in vivo and in vitro, of removing iron from transferrin.^{9,10} This kinetic barrier to iron removal can only be overcome by the addition of other anions to the system,¹¹ a phenomenon that appears to be shared by other hydroxamate-based compounds.

In contrast, enterobactin, a catechol-containing siderophore, is both thermodynamically and kinetically capable of iron removal from transferrin.^{12–14} Use of enterobactin as a drug for chelation therapy is unfortunately precluded by the extreme lability of the molecule itself.¹⁵ Recently we have engaged in the design and synthesis of catechol-based chelating agents modeled on enterobactin (Figure 1).^{1,16} We hoped that these molecules would retain the exceedingly high affinity of enterobactin for iron as well as the kinetic ability to remove iron from transferrin, but would prove more resistant to hydrolysis and oxidation. The results of the interaction of several of these model compounds with transferrin are reported herein.